Acta Crystallographica Section D
Biological Crystallography
ISSN 0907-4449

Structure of the human S100A12–copper complex: implications for host-parasite defence

O. V. Moroz,[a]* A. A. Antson,[a] S. J. Grist,[a] N. J. Maitland,[b] G. G. Dodson,[a,c] K. S. Wilson,[a] E. Lukanidin[d] and I. B. Bronstein[a]

[a]Department of Chemistry, University of York, York YO10 5YW, England, [b]Yorkshire Cancer Research Unit, Department of Biology, University of York, York YO10 5YW, England, [c]National Institute of Medical Research, Mill Hill, London NW7 1AA, England, and [d]Department of Molecular Cancer Biology, Institute for Cancer Biology, Danish Cancer Society, Strandboulevarden 49, Copenhagen 2100, Denmark

Correspondence e-mail: olga@ysbl.york.ac.uk

Received 13 December 2002
Accepted 27 February 2003

PDB Reference: S100A12–copper complex, 1odb, r1odbsf.

S100A12 is a member of the S100 family of EF-hand calcium-modulated proteins. Together with S100A8 and S100A9, it belongs to the calgranulin subfamily, *i.e.* it is mainly expressed in granulocytes, although there is an increasing body of evidence of expression in keratinocytes and psoriatic lesions. As well as being linked to inflammation, allergy and neuritogenesis, S100A12 is involved in host-parasite response, as are the other two calgranulins. Recent data suggest that the function of the S100-family proteins is modulated not only by calcium, but also by other metals such as zinc and copper. Previously, the structure of human S100A12 in low-calcium and high-calcium structural forms, crystallized in space groups $R3$ and $P2_1$, respectively, has been reported. Here, the structure of S100A12 in complex with copper (space group $P2_12_12$; unit-cell parameters a = 70.6, b = 119.0, c = 90.2 Å) refined at 2.19 Å resolution is reported. Comparison of anomalous difference electron-density maps calculated with data collected with radiation of wavelengths 1.37 and 1.65 Å shows that each monomer binds a single copper ion. The copper binds at an equivalent site to that at which another S100 protein, S100A7, binds zinc. The results suggest that copper binding may be essential for the functional role of S100A12 and probably the other calgranulins in the early immune response.

1. Introduction

S100A12 is a member of the S100 family of EF-hand calcium-modulated proteins, of which 21 members have been identified to date (reviewed in Heizmann *et al.*, 2002; Donato, 2001; Heizmann & Cox, 1998; McNutt, 1998; Schäfer & Heizmann, 1996; Zimmer *et al.*, 1995; Fano *et al.*, 1995; Kligman & Hilt, 1988). The S100 proteins contain two regions of high similarity, namely the two calcium-binding EF-hand motifs, and are associated with many human diseases including chronic inflammation, neurological disorders, and tumour growth and metastasis. Most S100 proteins are non-covalent homodimers. However, some homo- and hetero-assemblies have been reported (Isobe *et al.*, 1981; Edgeworth *et al.*, 1991; Réty *et al.*, 1999; Yang *et al.*, 1999; Deloulme *et al.*, 2000; Strupat *et al.*, 2000; Tarabykina *et al.*, 2000; Wang *et al.*, 2000; Gribenko *et al.*, 2001; Moroz *et al.*, 2002).

A calcium-sensor mechanism has been proposed for most of the S100 proteins, in which binding of calcium leads to significant conformational changes, resulting in the exposure of two hydrophobic target-binding surfaces per dimer (Chazin, 1995; Smith & Shaw, 1998). This has been strongly supported by the recently determined crystal structures of S100A6 in calcium-bound and calcium-free forms (Otterbein *et al.*, 2002).

Structures of S100A10 (Réty *et al.*, 1999), S100A11 (Réty *et al.*, 2000) and S100B (Rustandi *et al.*, 2000) complexes with the appropriate peptides have revealed the location of the target-binding sites. These are in good agreement with the location of the hydrophobic patches exposed when calcium is bound to S100A6. The binding sites are positioned on the opposite sides of the dimer, which probably enables the protein to bind two similar or even different targets at the same time.

However, not all S100 proteins bind calcium. The N-terminal EF-hand of S100A7 lacks three amino acids essential for calcium binding (Brodersen *et al.*, 1998) and S100A10 has calcium-free loops that are frozen in the 'calcium-bound' conformation (Réty *et al.*, 1999), while S100A3 has a very low affinity for calcium, possibly explained by deformation of the C-terminal EF-hand (Mittl *et al.*, 2002). It has been suggested that S100A3 and S100A7 are regulated by zinc (Fritz *et al.*, 2002; Brodersen *et al.*, 1999). Zinc binding to S100B was studied by UV-spectroscopy methods and zinc was shown to regulate calcium binding (Baudier *et al.*, 1986); several other S100 proteins have been reported to bind Zn^{2+} ions (reviewed in Heizmann & Cox, 1998).

The crystal structure of S100A7 revealed the location of the zinc-binding site, which is composed of an N-terminal histidine and an aspartic acid from one subunit and two C-terminal histidines from a second subunit. Sequence comparison showed that S100A8, S100A9, S100A12 and S100B could have similar zinc-binding sites (Brodersen *et al.*, 1999). Involvement of the C-terminal H*xxx*H motif of S100A8, S100A9 and S100A12 in zinc binding had been previously predicted on the basis of sequence alignment (Marti *et al.*, 1996). Different zinc-binding motifs (mostly cysteine-containing) were proposed for S100A2 (Stradal *et al.*, 2000; Randazzo *et al.*, 2001), S100A3 (Fritz *et al.*, 2002) and S100A5 (Schäfer *et al.*, 2000).

There is increasing evidence that some S100-family members can bind copper (Heizmann & Cox, 1998). S100B was identified as a copper-binding protein (Nishikawa *et al.*, 1997) and a role in protecting cells from copper-induced damage was proposed (Shiraishi & Nishikimi, 1998). Copper-dependent formation of disulfide-linked S100B dimers has been linked to nitric oxide production in microglial cell line BV2 (Lee *et al.*, 2000). Copper binds to S100A13, fibroblast growth factor 1 and synaptotagmin with similar affinity. In the presence of copper, these proteins form a multiprotein complex required for their release into the extracellular space (Landriscina *et al.*, 2001). For S100A5, copper binding was reported to be strongly antagonistic to calcium binding and it was suggested that copper could bind to some of the ligands from the EF-hand loops (Schäfer *et al.*, 2000). Fluorescence measurements of zinc and copper binding to the S100A8/S100A9 heterocomplex showed conformational changes induced by both metals. Interestingly, these were of different character, with zinc (at higher concentrations) increasing and copper decreasing the fluorescence intensity. While low concentrations of zinc decreased the fluorescence intensity, the fluorescence maximum was shifted, which did not occur for copper. While these observations indicated that Zn^{2+} and Cu^{2+} induced different conformational changes, both Zn^{2+} and Cu^{2+} prevented binding of arachidonic acid to the heterotetramer (Kerkhoff *et al.*, 1999).

S100A12 is a member of the calgranulin S100 subfamily (for a review, see Moroz *et al.*, 2003). It is expressed in granulocytes, as are two other calgranulins S100A8 and S100A9; expression in keratinocytes has also been reported (Gottsch & Liu, 1997, 1998). In addition, as with S100A7, S100A12 is expressed in psoriatic skin (Robinson & Hogg, 2000; Mirmohammadsadegh *et al.*, 2000, 2001).

The exact function of S100A12 is not yet known, but links with several important processes have been established. A cell-surface receptor for S100A12 (RAGE) has been identified on inflammatory cells and neurons: interaction of S100A12 with RAGE mediates inflammation (Hofmann *et al.*, 1999). Adding human recombinant S100A12 to cultured hippocampal cells induces neuritogenesis (Mikkelsen *et al.*, 2001). S100A12 as well as S100A13 binds the antiallergic drugs amlexanox, cromolyn and tranilast, suggesting the involvement of these proteins in allergic reaction (Shishibori *et al.*, 1999).

The most likely role of S100A12 established to date is in host–parasite response. Taken together, calgranulins S100A8, S100A9 and S100A12 comprise approximately 50% of neutrophil cytosolic proteins (Edgeworth *et al.*, 1991; Dell'Angellica *et al.*, 1994; Guignard *et al.*, 1995). Neutrophils provide the first line of defence against infection. Not surprisingly, calgranulins have been shown to have antimicrobial activity (Steinbakk *et al.*, 1990; Brandtzaeg *et al.*, 1995; Santhanagopalan *et al.*, 1995). For S100A8/S100A9 antimicrobial activity was linked to zinc binding, with depriving microorganisms of zinc as a possible mechanism (Clohessy & Golden, 1995; Sohnle, 1997; Sohnle *et al.*, 2000; Yui *et al.*, 2002). Antibacterial activity was shown for a 15-amino-acid peptide from the C-terminus of S100A12 (Cole *et al.*, 2001). In addition, antiparasite activity has been reported for all calgranulin-family members. An early role in immune response to *Onchocerca volvulus* has been proposed for S100A8/S100A9 based on the result of immunohistochemical analysis of onchocercal nodules (Edgeworth *et al.*, 1993). S100A12 is also involved in host–parasite response; it was purified from extracts of *O. volvulus* (Marti *et al.*, 1996) and shown to be associated with autoimmune corneal diseases related to invasion by filarial parasites (Gottsch, Li *et al.*, 1999; Gottsch, Eisinger *et al.*, 1999). However, the antiparasite activity of S100A12 is not the result of zinc sequestration (Gottsch, Eisinger *et al.*, 1999).

S100A12 has been shown to bind zinc (Dell'Angellica *et al.*, 1994) and the H*xxx*H zinc-binding motif was subsequently identified (Marti *et al.*, 1996). Recent results of electrospray mass spectrometry show that apart from zinc, S100A12 can bind copper (Burkitt *et al.*, 2003). Recent data indicate a significant role for copper in processes where S100 proteins are implicated (proliferation of human endothelial cells, angiogenesis; McAuslan & Gole, 1980; Hu, 1998; Rabinovitz, 1999; Sen *et al.*, 2002; Brewer, 2001). Moreover, copper seems to be of particular importance for the development and normal function of neutrophils (Percival, 1995; Karimbakas *et*

al., 1998). Despite its functional importance, very little is known about the binding of copper to the S100 proteins. Here, we report the crystal structure of S100A12 in complex with copper and discuss its possible functional role in the immune response.

2. Methods

2.1. Crystallization and data collection

Human cDNA of S100A12 was recloned from pQE30 into the pQE60 vector using *Bam*HI and *Hin*dIII cloning sites. This results in additional MGGS codons at the N-terminus and removal of the His tag from the pQE60 vector. Expressed protein was purified by phenyl-Sepharose and ResQ columns. Details of this chromatographic procedure are similar to those described for mouse S100A4 (Tarabykina *et al.*, 2000). Prior to crystallization, the purified protein was concentrated using a 10K ultrafiltration membrane (Filtron) to 5.0–8.0 mg ml^{-1} in 10 m*M* HEPES pH 7.3. The initial crystals were grown by the hanging-drop vapour-diffusion method. The reservoir contained 0.1 *M* sodium cacodylate pH 6.5, 250 m*M* NaCl, 5 m*M* $CaCl_2$, 1 m*M* $CuCl_2$ and 5–7% PEG 5K monomethyl ether (Brzozowski, 1993). Crystals grew as clusters of thin plates in around a week (Fig. 1*a*). Streak-seeding resulted in single crystals that grew overnight (Fig. 1*b*). S100A12–copper complex crystals were characterized using Cu $K\alpha$ X-rays from a Rigaku RU-200 rotating-anode generator. The crystals were vitrified at 120 K using an Oxford Cryosystems device. The cryoprotectant solution contained 10% PEG 5K monomethyl ether, 25% glycerol, 250 m*M* NaCl, 5 m*M* $CaCl_2$, 1 m*M* $CuCl_2$ and 0.1 *M* sodium cacodylate pH 6.5. Crystals belonged to space group $P2_12_12$, with unit-cell parameters a = 70.6, b = 119.0, c = 90.2 Å, and diffracted to 2.5–2.8 Å spacing in-house. There are six subunits of S100A12 in the asymmetric unit, resulting in a specific volume V_M of 3.0 Å^3 Da^{-1} and a solvent content of 58.3%. The zinc-containing crystals look totally different from those of the copper complex (Fig. 1*c*) and only diffract to very low resolution (around 8 Å), although the crystallization conditions for the zinc and copper complexes were essentially identical. The only difference is the presence of 1 m*M* $ZnCl_2$ in place of 1 m*M* $CuCl_2$ in the mother liquor.

Table 1
Statistics for the X-ray data.

Data set collected at EMBL, Hamburg; λ = 1.38 Å. The limited resolution of 3.5 Å was a consequence of crystal damage during transportation.

Resolution (Å)	No. of unique reflections	$\langle I/\sigma(I)\rangle$	$I/\sigma(I) > 3$ (%)	Completeness (%)	$R_{merge}(I)$ (%)
25.00–7.48	1105	15.8	91.8	99.1	7.3
7.48–5.96	1033	12.9	79.1	98.6	13.2
5.96–5.22	1026	11.4	80.0	99.0	15.2
5.22–4.74	1010	11.9	81.1	99.2	13.7
4.74–4.41	1009	11.7	83.2	99.0	13.1
4.41–4.15	992	10.5	80.1	99.2	14.3
4.15–3.94	1001	9.3	72.5	99.1	17.9
3.94–3.77	991	8.2	71.2	99.0	20.3
3.77–3.62	1000	7.6	68.3	98.7	21.3
3.62–3.50	984	5.4	59.8	98.9	29.7
All *hkl*	10151	11.0	77.0	99.0	14.0

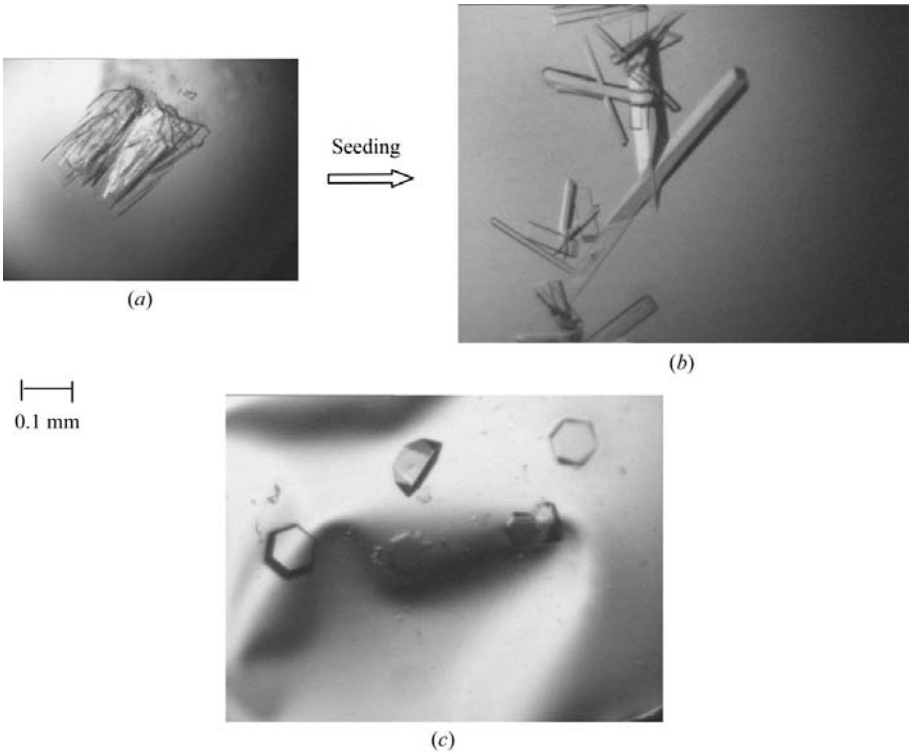

Figure 1
(*a*) Crystals of S100A12 grown in the presence of 1 m*M* $CuCl_2$. (*b*) Crystals of S100A12 in the presence of copper grown by streak seeding from (*a*). (*c*) Crystals of S100A12 grown in the presence of 1 m*M* $ZnCl_2$.

The initial 99% complete data set was collected using synchrotron radiation at EMBL Hamburg beamline BW7A, on the short-wavelength side of the copper edge (λ = 1.373 Å *versus* λ_{edge} = 1.38 Å). Unfortunately, the crystals had become damaged during transportation and only diffracted to 3.5 Å resolution. While these data were sufficient to indicate the binding of copper, they were not used for the refinement of the structure and are not described in detail here. The statistics for these data are summarized in Table 1. Data from a second crystal were collected at ESRF beamline BM14 at two wavelengths: 1.37 Å (close to the copper absorption edge) and 1.65 Å, which is above the copper edge and results in significant anomalous peaks at the calcium-ion sites (Fig. 3*a*). This experiment was undertaken to clarify whether copper is able to occupy calcium sites and *vice versa*, as an antagonism between these ions had been reported for S100A5 (Schäfer *et al.*,

Table 2
Statistics for the X-ray data collected at ESRF beamline BM14.

(*a*) Data set I, λ = 1.37 Å.

Resolution (Å)	No. of unique reflections	$\langle I/\sigma(I)\rangle$	$I/\sigma(I) > 3$ (%)	Completeness (%)	$R_{merge}(I)$† (%)
25.00–4.71	4176	23.6	97.6	99.6	4.1
4.71–3.74	4024	26.5	97.7	100	4.5
3.74–3.27	3996	22.3	97.1	100	6.0
3.27–2.97	3960	17.6	91.5	100	8.3
2.97–2.76	3932	14.6	85.9	100	11.1
2.76–2.60	3932	10.3	79.2	100	16.5
2.60–2.47	3913	8.7	72.3	100	20.1
2.47–2.36	3904	7.6	65.0	100	24.7
2.36–2.27	3905	5.7	57.3	100	31.1
2.27–2.19	3814	3.2	43.2	97.6	36.3
All *hkl*	39556	18.1	79.2	99.7	7.3

(*b*) Data set II, same crystal; λ = 1.65 Å.

Resolution (Å)	No. of unique reflections	$\langle I/\sigma(I)\rangle$	$I/\sigma(I) > 3$ (%)	Completeness (%)	$R_{merge}(I)$† (%)
25.00–5.26	2975	22.5	95.4	97.5	4.4
5.26–4.18	2881	22.6	96.5	99.2	5.7
4.18–3.66	2862	19.7	96.0	99.4	6.7
3.66–3.32	2851	16.7	95.7	99.9	8.1
3.32–3.09	2830	13.6	89.9	100.0	9.6
3.09–2.90	2823	10.8	82.8	100.0	12.5
2.90–2.76	2822	10.0	77.7	100.0	14.8
2.76–2.64	2821	7.6	70.4	100.0	20.1
2.64–2.54	2804	6.0	63.4	100.0	25.1
2.54–2.45	2757	4.1	53.5	98.1	28.5
All *hkl*	28426	16.5	82.3	99.4	7.7

† R_{merge} is defined as $100 \times \sum |I - \langle I\rangle| / \sum I$, where I is the intensity of the reflection.

2000). The data were processed with *DENZO* and *SCALEPACK* (Otwinowski & Minor, 1997).

The statistics for the two ESRF data sets are summarized in Table 2. Data set I (1.37 Å) was used for the refinement. Data set II (1.65 Å) was collected to lower resolution with shorter exposures and was only used for anomalous difference electron-density map calculation.

2.2. Structure determination and refinement

Crystallographic calculations were performed using the *CCP*4 program package (Collaborative Computational Project, Number 4, 1994). Molecular replacement using *MOLREP* (Vagin & Teplyakov, 1997) with the structure of the S100A12 dimer from the *R*3 crystal form (PDB entry 1e8a) as a search model gave three solutions for the three independent dimers in the asymmetric unit.

The structure was refined against data set I using *REFMAC* (Murshudov *et al.*, 1997). Initially, each monomer was treated as a rigid body. After convergence of rigid-body refinement, anomalous difference electron-density maps were calculated for both data sets. In order to avoid bias, the occupancies for calcium ions in the coordinate file were set to zero. The map for data set II (1.65 Å) showed peaks at about the 8σ level for calcium ions in the calcium-binding EF-hand loops, while the map for data set I (1.37 Å, near the copper edge) showed another set of peaks at about 22σ, corresponding to bound Cu atoms. There was one copper peak per monomer (six per asymmetric unit) in the predicted copper/zinc-binding site. The six copper ions were added to the model.

Table 3
Model refinement statistics.

Resolution limits (Å)	25.0–2.19
Total No. of reflections	37532
Percentage observed	99.53
Percentage of free reflections	5
R_{cryst}† (%)	18.6
Free *R* factor (%)	22.6
ESU for positional parameters (Å)	0.13
Cruickshank's DPI for coordinate errors (Å)	0.20
R.m.s. deviations from ideal geometry‡	
Bond distances (Å)	0.014 (0.021)
Bond angles (°)	1.353 (1.927)
Chiral centres (Å^3)	0.086 (0.20)
Planar groups (Å)	0.004 (0.020)
Main-chain bond *B* values (Å^2)	0.53 (1.50)
Main-chain angle *B* values (Å^2)	0.96 (2.00)
Side-chain bond *B* values (Å^2)	1.72 (3.00)
Side-chain angle *B* values (Å^2)	2.83 (4.50)
Mean temperature factor *B* (Å^2)	
Main chain	45.7
Side chain + waters	48.9
Calcium ions	39.7
Copper ions	37.5

† $R_{cryst} = \sum \big||F_o| - |F_c|\big| / \sum |F_o|$. ‡ Values in parentheses are target values.

Individual atomic refinement was conducted with NCS restraints (tight restraints for the main chain, loose restraints for the side chains). The resulting map was averaged with *MAPROT* and manual rebuilding was performed using the *XFIT* (Oldfield, 1994) option of the program *QUANTA* (Molecular Simulations, Inc.). For further refinement, the TLS option (Schomaker & Trueblood, 1968; Winn *et al.*, 2001) was used to account for overall anisotropic motion of the monomers. The NCS restraints were first changed to medium for the main chain and loose for side chains. When the R/R_{free} values had fallen to 20.8/25.0%, refinement was continued without NCS restraints. From this stage onwards, model rebuilding was performed separately for each independent monomer. Solvent positions were added using *ARP*/*wARP* (Lamzin & Wilson, 1997) alternated with *REFMAC*. Finally, the contribution of the H atoms to the structure factors was taken into account: this led to a drop of R/R_{free} values from 19.1/23.6% to 18.6/22.6%. The results of refinement are summarized in Table 3.

2.3. Sequence analysis

Multiple sequence alignments were performed using the *CLUSTALW* service at the European Bioinformatics Institute (http://www.ebi.ac.uk/clustalw; Higgins *et al.*, 1996); all the sequences were extracted from SWISS-PROT protein database in FASTA format.

3. Results and discussion

3.1. Quality of the refined model

The structure of the S100A12–copper complex has been refined to an *R* factor of 18.6% for all data in the resolution range 25–2.19 Å, excluding the randomly distributed 5% of

reflections assigned to calculate R_{free} (22.6%). There are three dimers in the asymmetric unit, composed of subunits *A*/*B*, *C*/*D* and *E*/*F*. The final electron-density map allowed positioning of residues 1–90 for chains *A*–*E* and residues 1–89 for chain *F*. There was also electron density for Ser0, which is the first of four extra N-terminal residues in this construct. There was no significant electron density for several surface residues, mostly lysines from linker loops 41–51; the most poorly defined is the linker loop of the subunit *F*. The model contains 9980 atoms including 12 Ca atoms, six Cu atoms and 374 water molecules. All residues are in the allowed regions of the Ramachandran plot (Ramakrishnan & Ramachandran, 1965), with 92.3% in the most favoured regions (Fig. 2).

3.2. Copper and calcium: anomalous peaks

The anomalous difference electron-density maps of the two data sets are very different at the metal-binding sites. The map for data set II (1.65 Å) showed clear peaks at the 7.7σ level for calcium ions in the calcium-binding EF-hand loops, while the map for data set I (1.37 Å, near the copper edge) showed peaks at 21.9σ at sites distant from Ca atoms, corresponding to bound Cu atoms. The average ratio of 2.9 between peak heights corresponds well to the theoretical ratio of 2.7 between the f'' contributions for copper at 1.37 Å and for calcium at 1.65 Å (Fig. 3*a*). The data show that calcium and copper bind to S100A12 at distinct binding sites (Fig. 3*b*).

The copper ion is coordinated by His15 and Asp25 from one subunit of the dimer and by His85 and His89 from the other subunit (Fig. 4). The bond lengths (Table 3) are in good agreement with the average values for copper–ligand distances (Harding, 2001). Five of the six copper ions per asymmetric unit are coordinated in an identical manner. The sixth copper lies at the *A*/*B* interface and differs somewhat in its coordination; this is most probably an artefact of crystal packing as this site is coordinated by Glu55 from chain *E* (belonging to a symmetry-related molecule) instead of Asp25. The coordination distance is 2.4 Å, which is slightly longer than normal and the distance to His85 is also longer than usual. This abnormal copper-binding site was not included in the average ligand-distance calculation (Table 4).

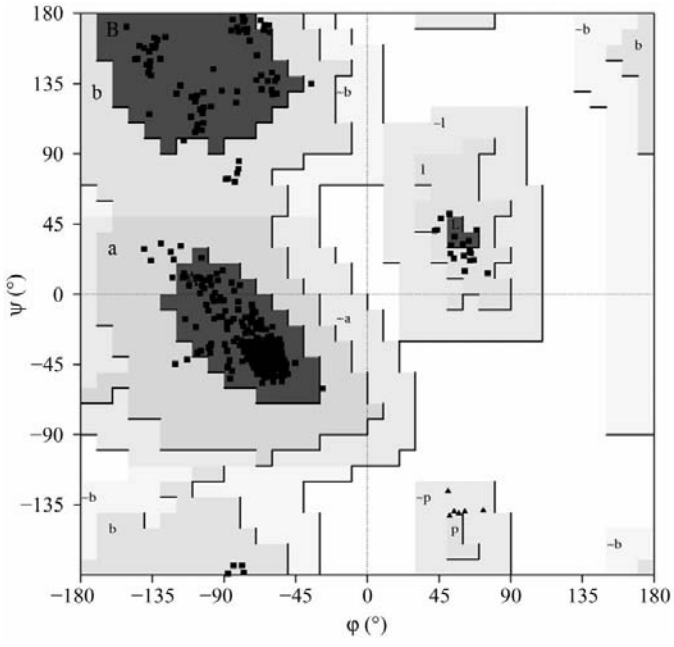

Figure 2
Ramachandran plot for six independent subunits of S100A12–copper complex calculated using *PROCHECK* (Laskowski *et al.*, 1993).

Table 4
Copper–ligand bond distances.

The distances shown are average values for five Cu-binding sites; site *A*/*B* was not included because of abnormal copper coordination; stdev is the standard deviation from the average value.

Bond	Cu—N$^{\varepsilon}$ (His15)	Cu—O$^{\varepsilon 1}$ (Asp25)	Cu—N$^{\varepsilon}$ (His85)	Cu—N$^{\varepsilon}$ (His89)
Distance (Å)	2.06	2.05	2.01	2.04
stdev	0.04	0.02	0.05	0.04

3.3. Structural comparison

The structure of the Cu^{2+}-binding site is closely similar to that of the zinc-binding site of S100A7. Sequence alignment of S100A8, S100A9 and S100B from different species shows that all of them have similar putative zinc/copper-binding sites,

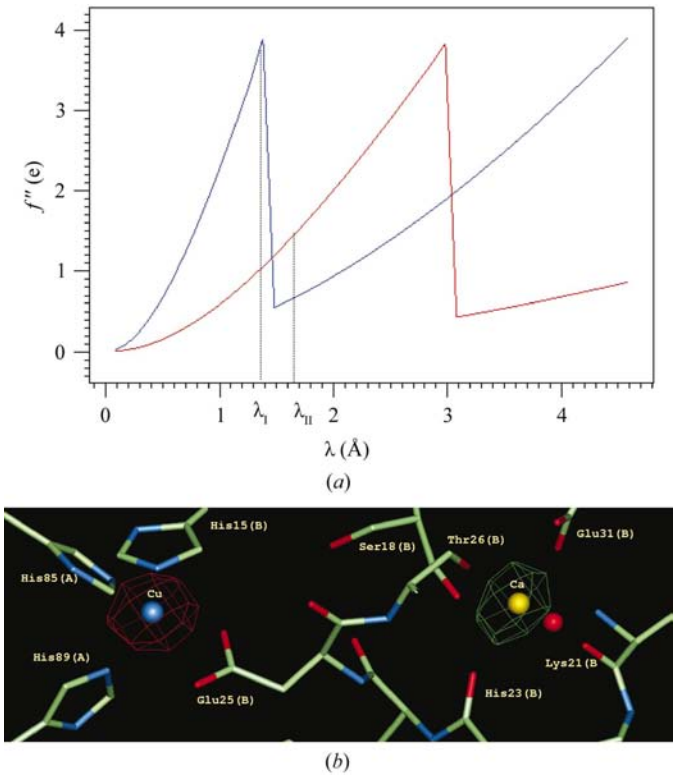

Figure 3
(*a*) $f''(\lambda)$ plots for copper (in blue) and for calcium (in red). Dotted lines correspond to the wavelengths for set I (λ_I = 1.37 Å) and for data set II (λ_{II} = 1.65 Å). (*b*) Anomalous difference electron-density maps for data sets I (λ = 1.37 Å) and II (λ = 1.65 Å). Electron density for data set I is contoured at the 10σ level and is shown in red. Electron density for data set II is contoured at the 5σ level and is shown in green. This figure and Fig. 4 were generated using *QUANTA* (Molecular Simulations, Inc.).

usually composed of three histidines and one aspartate (Fig. 5). Deviations in coordination occur in S100A8 (four histidines) and S100B (histidine instead of Asp25 and glutamate instead of His89). Structural comparison shows that the zinc/copper-binding sites are very similar for all these proteins (Fig. 6). Residues corresponding to Asp25 in the S100A12 structure have their side chains turned away from the metal-binding sites in metal-free proteins, while in the structures of metal-bound S100 proteins they point towards the metal and make a monodentate (S100A12) or a bidentate (S100A7) bond with it. Two C-terminal metal-binding residues are not visible in the structure of S100A9; neither is Glu89 in the S100B structure. Therefore, structural comparisons for them are not possible. However, the C-terminus including His89 was also disordered for S100A12 in the copper-free form and only became visible in the copper-bound structure. It seems likely that the C-termini of S100A9 and S100B would also become ordered upon metal binding, although this can only be confirmed after the three-dimensional structures of copper or zinc complexes of these proteins are determined. However, the N-terminal residues of S100B and S100A9 overlap well with the others. The copper-binding site is located close to the surface of the S100 proteins and to their putative target-binding site, suggesting that it is functionally important.

Polyhistidine copper chelation is typical for that observed in type II copper centres. The usual configuration of the type II copper centre is $Cu(N^{\varepsilon}_{His})_m R_n$, where m = 1–4, n = 0–3 and R is an O or S atom. The usual geometry for type II copper centres is either planar or tetrahedral; it is close to tetrahedral in S100A12. A search in the metalloprotein database (Castagnetto *et al.*, 2002) for four ligands with at least three His and no more than one Asp/Glu gave 85 hits, the majority of which were oxidoreductases. Refining the search to 'at least one Asp/Glu' gave only the copper-containing nitrite reductase from *Alcaligenes faecalis*, in which the copper is coordinated by three histidines and a water molecule, but there is a functionally important Asp in the vicinity of the active site (Murphy *et al.*, 1997). In addition, copper coordination by three histidines plus a carboxylic acid and a water molecule was recently reported for the copper-containing quercitin 2,3-oxygenase (Fusetti *et al.*, 2002), not yet incorporated in the metalloprotein database. The results of the search raise the possibility of oxidoreductase activity for S100A12 and possibly for all the calgranulin subfamily. However, more extensive structural comparisons will be required to support this hypothesis. Conducting several activity assays is clearly needed to draw final conclusions on S100A12 function, but these are not

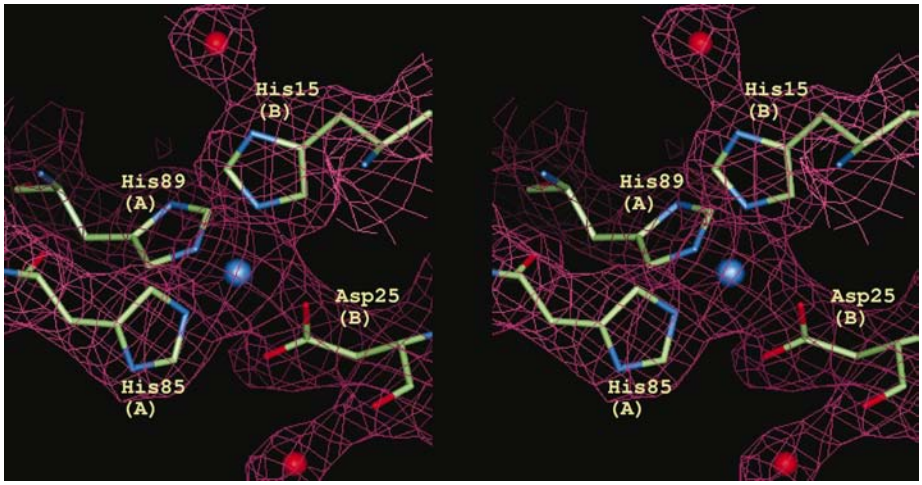

Figure 4
Stereoview of the electron density for the region of the copper-binding site overlapped with the final model; likelihood-weighted $2|F_o| - |F_c|$ electron-density map contoured at 1 r.m.s. deviation above the mean density level (0.172 e Å^{-3}). The copper ion is in blue and the water molecules are in red.

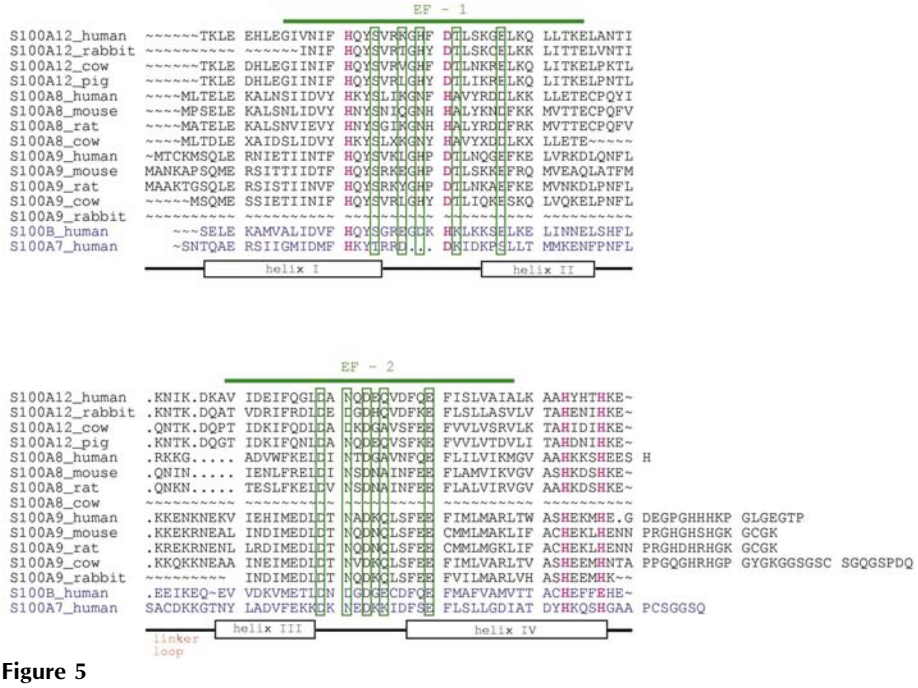

Figure 5
Sequence alignment of all known members of calgranulin subfamily together with human S100A7 and S100B. α-Helical regions are shown by boxes and calcium-binding EF-hand regions are indicated by thick green lines. Residues binding calcium are outlined with green boxes. Zinc/copper-binding residues are shown in red. Non-calgranulin human S100A7 and S100B sequences are in blue. The sequences were obtained from the SWISS-PROT protein-sequence database. Multiple sequence alignment was performed using the *CLUSTALW* service at the European Bioinformatics Institute (http://www.ebi.ac.uk/clustalw; Higgins *et al.*, 1996).

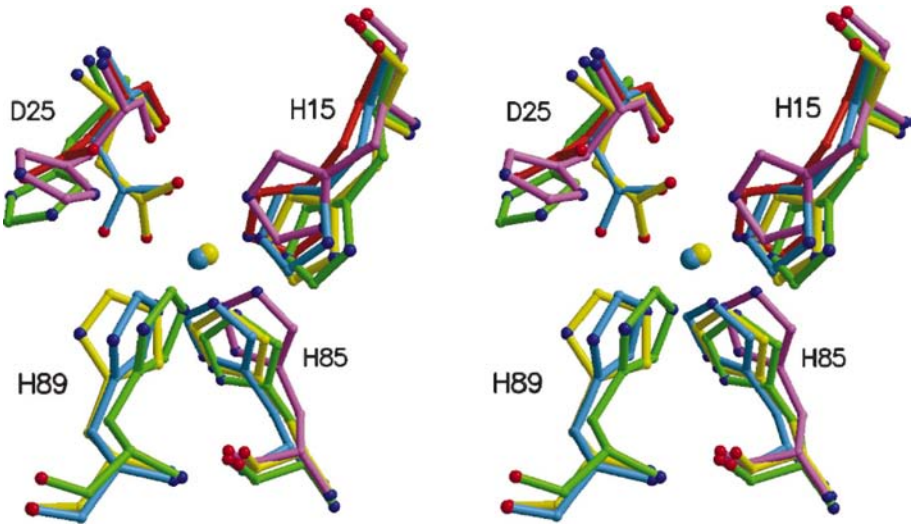

Figure 6
Superposition of the copper-binding site of S100A12 (PDB code 1odb), the zinc-binding site of S100A7 (2psr) and corresponding regions of S100A8 (1mr8), S100A9 (1irj) and S100B (1mho) shown in ball-and-stick representation. S100A12 is shown in blue, S100A8 in green, S100A9 in orange, S100A7 in yellow and S100B in violet. Copper ion from the S100A12–copper complex structure is in blue, zinc ion from the S100A7–zinc complex is in yellow. The figure was generated using *MOLSCRIPT* (Kraulis, 1991) and *Raster3D* (Merritt & Murphy, 1994).

straightforward because of some degree of non-specific copper binding to additional binding sites and the high redox activity of this transition metal even when it is not bound to the protein.

3.4. Changes in the S100A12 structure upon copper binding

The structure of the S100A12 dimer in complex with copper is in general similar to those of the S100A12 dimers in the low-calcium (space group $R3$) and high-calcium (space group $P2_1$) structural states. However, there are considerable changes at the C-terminus, where clear electron density appears for four residues that were not seen before, with the α-helix now extending to Lys90. These four residues include the copper-binding His89, which was invisible in the copper-free structures. Thus, the conformation of the putative target-binding site, consisting of the N-terminus, the linker loop and the C-terminus (Moroz *et al.*, 2001), changes significantly. The conformation of the N-terminal EF-hand, however, remains essentially the same, with the r.m.s.$_{xyz}$ deviation between the main-chain atoms of the copper complex and the $R3$ structure being 0.267 Å for subunit *A* and 0.337 Å for subunit *B* (calculated for the EF-1 consensus motif; *i.e.* residues 9–40). This is similar to the r.m.s. deviation between subunits *A* and *B* from the same structure. This shows that in contrast to the situation reported for S100A5 (Schäfer *et al.*, 2000), there is no antagonism between calcium and copper binding to S100A12. This observation is supported by the mass-spectrometric results (Burkitt *et al.*, 2003)

4. Conclusions

Sequence alignment shows that the calgranulins S100B and S100A7 have a zinc/copper-binding motif which is highly conserved in all known species (Fig. 5). There is (as expected) a high structural similarity for these proteins in this region. Until now, functionally relevant copper-binding has been reported only for one member of this group, S100B, for which a role in copper sequestration was proposed (Shiraishi & Nishikami, 1998).

For the calgranulins S100A8, S100A9 and S100A12, no copper-related function has been reported. Nevertheless, a direct link between copper and the immune response has been established (Percival, 1998). The number of neutrophils in human peripheral blood is reduced in cases of copper deficiency; moreover, their ability to generate superoxide and kill ingested microorganisms is impaired. Neutrophil-like cells HL-60 that acquire mature neutrophil characteristics when incubated with retinoic acid were shown to accumulate copper. This accumulation was not accounted for by changes in the activity of known copper-binding proteins such as superoxide dismutase and cytochrome *c* oxidase, suggesting the presence of as yet unidentified additional copper-binding proteins. The abundance of calgranulins in neutrophils and their implication in antimicrobial and antiparasite activity together with structural information gives reason to suppose that these unknown copper-binding proteins are S100A8/S100A9 and S100A12. It is possible that calgranulins are released by granulocytes to combat parasites and microorganisms and that one of the mechanisms could be copper-mediated generation of reactive oxygen species such as superoxide ions, hydrogen peroxide, hypochlorite or hydroxyl ions. The observation that the antimicrobial activity of S100A8/S100A9 is zinc-reversible (Sohnle *et al.*, 2000) could be explained by zinc substituting copper in the zinc/copper-binding sites of calgranulins, thus rendering them redox-inactive. In conclusion, our results support the hypothesis of copper binding being essential for the activity of calgranulins in the early immune response.

This work was funded by the Yorkshire Cancer Research grant No. Y242 and the Danish Cancer Society. We thank the BBSRC for financial support to the infrastructure of the York Structural Biology Laboratory, contract No. 87/SB09829 (UK). We thank the European Community for supporting work at the EMBL, Hamburg through Access to Research Infrastructure Action of the Improving Human Potential Programme to the EMBL Hamburg Outstation, contract No. HPRI-CT-1999-00017. We thank the staff of EMBL Hamburg and ESRF (beamline BM14) for provision of synchrotron facilities.

References

Baudier, J., Glasser, N. & Gerard, D. (1986). *J. Biol. Chem.* **261**, 8192–8203.

Brandtzaeg, P., Gabrielsen, T. O., Dale, L., Muller, F., Steinbakk, M. & Fagerhol, M. K. (1995). *Adv. Exp. Med. Biol.* **371**A, 201–206.

Brewer, G. J. (2001). *Exp. Biol. Med.* **226**, 665–673.

Brodersen, D. E., Etzerodt, M., Madsen, P., Celis, J. E., Thogersen, H. C., Nyborg, J. & Kjeldgaard, M. (1998). *Structure*, **6**, 477–489.

Brodersen, D. E., Nyborg, J. & Kjeldgaard, M. (1999). *Biochemistry*, **38**, 1695–1704.

Brzozowski, A. M. (1993). *Acta Cryst.* D**49**, 352–354.

Burkitt, W. I., Moroz, O. V., Grist, S. J., Bronstein, I. B. & Derrick, P. J. (2003). In preparation.

Castagnetto, J. M., Hennessy, S. W., Roberts, V. A., Getzoff, E. D., Tainer, J. A. & Pique, M. E. (2002). *Nucleic Acids Res.* **30**, 379–382.

Chazin, W. J. (1995). *Nature Struct. Biol.* **2**, 707–710.

Clohessy, P. A. & Golden, B. E. (1995). *Scand. J. Immunol.* **42**, 551–556.

Cole, A. M., Kim, Y.-H., Tahk, S., Hong, T., Weis, P., Waring, J. A. & Ganz, T. (2001). *FEBS Lett.* **504**, 5–10.

Collaborative Computational Project, Number 4 (1994). *Acta Cryst.* D**50**, 760–763.

Dell'Angelica, E. C., Schleicher, C. H. & Santome, J. A. (1994). *J. Biol. Chem.* **269**, 28929–28936.

Deloulme, J. C., Assard, N., Mbele, G. O., Mangin, C., Kuwano, R. & Baudier, J. (2000). *J. Biol. Chem.* **275**, 35302–35310.

Donato, R. (2001). *Int. J. Biochem. Cell B*, **33**, 637–668.

Edgeworth, J. D., Abiose, A. & Jones, B. R. (1993). *Clin. Exp. Immunol.* **92**, 84–92.

Edgeworth, J., Gorman, M, Bennett, R., Freemont, P. & Hogg, N. (1991). *J. Biol. Chem.* **266**, 7706–7713.

Fano, G., Biocca, S., Fulle, S., Mariggio, M. A., Belia, S. & Calissano, P. (1995). *Prog. Neurobiol.* **46**, 71–82.

Fritz, G., Mittl, P. R., Vasak, M., Grutter, M. G. & Heizmann, C. W. (2002). *J. Biol. Chem.* **277**, 33092–33098.

Fusetti, F., Schröter, K. H., Steiner, R. A., van Noort, P. I., Pijning, T., Rozenboom, H. J., Kalk, K. H., Egmond, M. R. & Dijkstra, B. W. (2002). *Structure*, **10**, 259–268.

Gottsch, J. D., Eisinger, S. W., Liu, S. H. & Scott, A. L. (1999). *Infect. Immun.* **67**, 6631–6636.

Gottsch, J. D., Li, Q., Ashraf, F., O'Brien, T. P., Stark, W. J. & Liu, S. H. (1999). *Clin. Immunol.* **91**, 34–40.

Gottsch, J. D. & Liu, S. H. (1997). *Curr. Eye Res.* **16**, 1239–1244.

Gottsch, J. D. & Liu, S. H. (1998). *Curr. Eye Res.* **17**, 870–874.

Gribenko, A. V., Hopper, J. E. & Makhatadze, G. I. (2001). *Biochemistry*, **40**, 15538–15548.

Guignard, F., Mauel, J. & Markert, M. (1995). *Biochem. J.* **309**, 395–401.

Harding, M. M. (2001). *Acta Cryst.* D**57**, 401–411.

Heizmann, C. W. & Cox, J. A. (1998). *Biometals*, **11**, 383–397.

Heizmann, C. W., Fritz, G. & Schafer, B. W. (2002). *Front. Biosci.* **7**, 1356–1368.

Higgins, D. G., Thompson, J. D. & Gibson, T. J. (1996). *Methods Enzymol.* **266**, 383–402.

Hofmann, M. A., Drury, S., Fu, C., Qu, W., Taguchi, A., Lu, Y., Avila, C., Kambham, N., Bierhaus, A., Nawroth, P., Neurath, M. F., Slattery, T., Beach, D., McClary, J., Nagashima, M., Morser, J., Stern, D. & Schmidt, A. M. (1999). *Cell*, **97**, 889–901.

Hu, G. F. (1998). *J. Cell Biochem.* **69**, 326–335.

Isobe, T., Ishioka, N. & Okuyama, T. (1981). *Eur. J. Biochem.* **115**, 469–474.

Karimbakas, J., Langkamp-Henken, B. & Percival, S. S. (1998). *J. Nutr.* **128**, 1855–1860.

Kerkhoff, C., Vogl, T., Nacken, W., Sopalla, C. & Sorg, C. (1999). *FEBS Lett.* **460**, 134–138.

Kligman, D. & Hilt, D. C. (1988). *Trends Biochem. Sci.* **13**, 437–442.

Kraulis, P. (1991). *J. Appl. Cryst.* **24**, 946–950.

Lamzin, V. S. & Wilson, K. S. (1997). *Methods Enzymol.* **277**, 269–305.

Landriscina, M., Bagala, C., Mandinova, A., Soldi, R., Micucci, I., Bellum, S., Prudovsky, I. & Maciag, T. (2001). *J. Biol. Chem.* **276**, 25549–25557.

Laskowski, R. A., MacArthur, M. W., Moss, D. S. & Thornton, J. M. (1993). *J. Appl. Cryst.* **26**, 283–291.

Lee, I. S. M., Suzuki, M., Hayashi, N., Hu, J., Van Eldik, L. J., Titani, K. & Nishikimi, M. (2000). *Arch. Biochem. Biophys.* **374**, 137–141.

McAuslan, B. R. & Gole, G. A. (1980). *Trans. Opthalmol. Soc. UK*, **100**, 354–358.

McNutt, N. S. (1998). *J. Cutan. Pathol.* **25**, 521–529.

Marti, T., Erttmann, K. D. & Gallin, M. Y. (1996). *Biochim. Biophys. Res. Commun.* **221**, 454–458.

Merritt, E. A. & Murphy, M. E. P. (1994). *Acta Cryst.* D**50**, 869–873.

Mikkelsen, S. E., Novitskaya, V., Kriajevska, M., Berezin, V., Bock, E., Norrild, B. & Lukanidin, E. (2001). *J. Neurochem.* **79**, 767–776.

Mirmohammadsadegh, A., Tschakarjan, E., Dexling, B. & Hengge, U. (2001). *J. Invest. Dermatol.* **117**, 741.

Mirmohammadsadegh, A., Tschakarjan, E., Ljoljic, A., Bohner, K., Michel, G., Ruzicka, T., Goos, M. & Hengge, U. R. (2000). *J. Invest. Dermatol.* **114**, 1207–1208.

Mittl, P. R., Fritz, G., Sargent, D. F., Richmond, T. J., Heizmann, C. W. & Grutter, M. G. (2002). *Acta Cryst.* D**58**, 1255–1261.

Moroz, O. V., Antson, A. A., Dodson, E. J., Burrell, H. J., Grist, S. J., Lloyd, R. M., Maitland, N. J., Dodson, G. G., Wilson, K. S., Lukanidin, E. & Bronstein, I. B. (2002). *Acta Cryst.* D**58**, 407–413.

Moroz, O. V., Antson, A. A., Murshudov, G. N., Maitland, N. J., Dodson, G. G., Wilson, K. S., Skibshøj, I., Lukanidin, E. & Bronstein, I. B. (2001). *Acta Cryst.* D**57**, 20–29.

Moroz, O. V., Dodson, G. G., Wilson, K. S., Lukanidin, E. & Bronstein, I. B. (2003). In the press.

Murphy, M. E., Turley, S. & Adman, E. T. (1997). *J. Biol. Chem.* **272**, 28455–28460.

Murshudov, G. N., Vagin, A. A. & Dodson, E. J. (1997). *Acta Cryst.* D**53**, 240–255.

Nishikawa, T., Lee, M. S. I., Shiraishi, N., Ishikawa, T., Ohta, Y. & Nishikimi, M. (1997). *J. Biol. Chem.* **272**, 23037–23041.

Oldfield, T. J. (1994). *Proceedings of the CCP4 Study Weekend. From First Map To Final Model*, edited by S. Bailey, R. Hubbard & D. A. Waller, pp 15–18. Warrington: Daresbury Laboratory.

Otterbein, L. R., Kordowska, J., Witte-Hoffmann, C., Wang, C. L. & Dominguez, R. (2002). *Structure*, **10**, 557–567.

Otwinowski, Z. & Minor, W. (1997). *Methods Enzymol.* **276**, 307–326.

Percival, S. S (1995). *Nutr. Rev.* **53**, 59–66.

Percival, S. S. (1998). *Am. J. Clin. Nutr.* **67**, 1064S–1068S.

Rabinovitz, M. (1999). *J. Natl Cancer Inst.* **91**, 1689–1690.

Ramakrishnan, C. & Ramachandran, G. N. (1965). *Biophys. J.* **5**, 909–933.

Randazzo, A., Acklin, C., Schafer, B. W., Heizmann, C. W. & Chazin, W. J. (2001). *Biochem. Biophys. Res. Commun.* **288**, 462–467.

Réty, S., Osterloh, D., Arie, J.-P., Tabaries, S., Seeman, J., Russo-Marie, F., Gerke, V. & Lewit-Bentley, A. (2000). *Structure*, **8**, 175–184.

Réty, S., Sopkova, J., Renouard, M., Osterloh, D., Gerke, V., Tabaries, S., Russo-Marie, F. & Lewit-Bentley, A. (1999). *Nature Struct. Biol.* **6**, 89–95.

Robinson, M. J. & Hogg, N. (2000). *Biochem. Biophys. Res. Commun.* **275**, 865–870.

Rustandi, R. R., Baldisseri, D. M. & Weber, D. (2000). *Nature Struct. Biol.* **7**, 570–574.

Santhanagopalan, V., Hahn, B. L. & Sohnle, P. G. (1995). *J. Infect. Dis.* **171**, 1289–1294.

Schäfer, B. W., Fritschy, J. M., Murmann, P., Troxler, H., Durussel, I., Heizmann, C. W. & Cox, J. A. (2000). *J. Biol. Chem.* **275**, 30623–30630.

Schäfer, B. W. & Heizmann, C. W. (1996). *Trends Biochem. Sci.* **21**, 134–140.

Schomaker, V. & Trueblood, K. N. (1968). *Acta Cryst.* B**24**, 63–76.

Sen, C. K., Khanna, S., Venojarvi, M., Trikha, P., Ellison, E. C., Hunt, T. K. & Roy, S. (2002). *Am. J. Physiol. Heart Circ. Physiol.* **282**, H1821–H1827.
Shiraishi, N. & Nishikimi, M (1998). *Arch. Biochem. Biophys.* **357**, 225–230.
Shishibori, T., Oyama, Y., Matsushita, O., Yamashita, K., Furuichi, H., Okabe, A., Maeta, H., Hata, Y. & Kobayashi, R. (1999). *Biochem. J.* **338**, 583–589.
Smith, S. P. & Shaw, G. S. (1998). *Biochem. Cell. Biol.* **76**, 324–333.
Sohnle, P. G. (1997). *Rev. Med. Microbiol.* **8**, 217–224.
Sohnle, P. G., Hunter, M. J., Hahn, B. & Chazin, W. J. (2000). *J. Infect. Dis.* **182**, 1272–1275.
Steinbakk, M., Naessandresen, C. F., Lingaas, E., Dale, I., Brandtzaeg, P. & Fagerhol, M. K. (1990). *Lancet*, **336**, 763–765.
Stradal, T. B., Troxler, H., Heizmann, C. W. & Gimona, M. (2000). *J. Biol. Chem.* **275**, 13219–13227.
Strupat, K., Rogniaux, H., Dorsselaer, A. V., Roth, J. & Vogl, T. (2000). *J. Am. Soc. Mass Spectrom.* **11**, 780–788.
Tarabykina, S., Kriajevska, M., Scott, D. J., Hill, T. J., Lafitte, D., Derrick, P. J., Dodson, G. G., Lukanidin, E. & Bronstein, I. B. (2000). *FEBS Lett.* **475**, 187–191.
Vagin, A. A. & Teplyakov, A. (1997). *J. Appl. Cryst.* **30**, 1022–1025.
Wang, G., Rudland, P. S., White, M. R. & Barraclough, R. (2000). *J. Biol. Chem.* **275**, 11141–11146.
Winn, M. D., Isupov, M. & Murshudov, G. N. (2001). *Acta Cryst.* D**57**, 122–133.
Yang, Q., O'Hanlon, D., Heizmann, C. W. & Marks, A. (1999). *Exp. Cell. Res.* **246**, 501–509.
Yui, S., Nakatani, Y., Hunter, M. J., Chazin, W. J. & Yamazaki, M. (2002). *Mediators Inflamm.* **11**, 165–172.
Zimmer, D. B, Cornwall, E. Y., Landar, A. & Song, W. (1995). *Brain Res. Bull.* **37**, 417–429.